Japanese Journal of Applied Physics

The Japan Society of Applied Physics

ACCEPTED MANUSCRIPT

Mg implantation in AlN layers on sapphire substrates

To cite this article before publication: hironori okumura *et al* 2023 *Jpn. J. Appl. Phys.* in press https://doi.org/10.35848/1347-4065/acb898

Manuscript version: Accepted Manuscript

Accepted Manuscript is "the version of the article accepted for publication including all changes made as a result of the peer review process, and which may also include the addition to the article by IOP Publishing of a header, an article ID, a cover sheet and/or an 'Accepted Manuscript' watermark, but excluding any other editing, typesetting or other changes made by IOP Publishing and/or its licensors"

This Accepted Manuscript is **© 2023 The Japan Society of Applied Physics**.

During the embargo period (the 12 month period from the publication of the Version of Record of this article), the Accepted Manuscript is fully protected by copyright and cannot be reused or reposted elsewhere.
As the Version of Record of this article is going to be / has been published on a subscription basis, this Accepted Manuscript is available for reuse under a CC BY-NC-ND 3.0 licence after the 12 month embargo period.

After the embargo period, everyone is permitted to use copy and redistribute this article for non-commercial purposes only, provided that they adhere to all the terms of the licence https://creativecommons.org/licences/by-nc-nd/3.0

Although reasonable endeavours have been taken to obtain all necessary permissions from third parties to include their copyrighted content within this article, their full citation and copyright line may not be present in this Accepted Manuscript version. Before using any content from this article, please refer to the Version of Record on IOPscience once published for full citation and copyright details, as permissions will likely be required. All third party content is fully copyright protected, unless specifically stated otherwise in the figure caption in the Version of Record.

View the article online for updates and enhancements.

This content was downloaded from IP address 133.51.188.70 on 03/02/2023 at 00:10

Mg implantation in AlN layers on sapphire substrates

Hironori Okumura[1,*] and Akira Uedono[1]

1 Faculty of Pure and Applied Sciences, University of Tsukuba, Tsukuba, Ibaraki 305-8573 Japan

[*]E-mail: okumura.hironori.gm@u.tsukuba.ac.jp

Mg ions were implanted in 1-μm-thick AlN layers grown on sapphire substrates. The Mg implantation with a total dose of 5×10^{14} cm^{-2} introduced Al-vacancy related defects, which were decreased by annealing at temperatures over 1400°C in a N_2 ambient. We found that annealing temperatures over 1400°C were necessary for an electrically conductive Mg-implanted AlN layer. The Mg-implanted AlN layer annealed at 1500ºC showed 1.1 nA at a bias of 100 V at room temperature and 7 nA at a bias of 10 V at 300ºC.

Accepted Manuscript

AlN is a much attractive material for ultra-violet light-emitting diodes and high-power devices due to its high critical electric field and large band-gap energy.[1)] AlN-channel devices including light-emitting diodes,[2)] Schottky-barrier diodes,[3-5)] and field-effect transistors,[6,7)] have been reported. Still, AlN-based devices suffer from high contact resistances due to a high Schottky barrier,[8,9)] large ionization energy,[10-12)] and formation of compensation defects.[13,14)] The contact resistances can be reduced by high-temperature sintering of a metal stack,[15)] an AlGaN-graded contact layer,[16,17)] a GaN contact layer,[18-20)] and heavy doping of the top-most AlN surfaces.[21)] In particular, selective doping just under the contacts would improve the performance of existing AlN devices.

High-dose ion implantation enables selective doping over 10^{19} cm^{-3}. Si-implanted AlN layers with doses over 10^{14} cm^{-2} show *n*-type conductance after annealing at temperatures over 1200°C in a N_2 ambient.[22-24)] However, there are the limited reports on *p*-type AlN layers formed using implantation technology. The major candidates of acceptor impurities in AlN are Be, Zn, and Mg. Although the Be acceptor has a small ionization energy of 340 meV,[25)] Be metal is harmful to human lungs and contaminates the implantation equipment. Mg acceptors have a smaller ionization energy than Zn acceptors.[2,26,27)] Thus, Mg is the most suitable acceptor for practical AlN devices. Electrical activation of implanted AlN layers requires a post-thermal annealing process to reduce implantation-induced damage, which causes compensation defects. Recently, we found that Mg atoms diffused deeply in the AlN layer after annealing at 1600°C.[24)] Dopant diffusion causes smaller carrier concentrations than expected as well as leakage current in unexpected areas. For electrically conductive AlN layers to be made using Mg implantation, we need to optimize the annealing temperatures to reduce implantation-induced damage while keeping steep Mg profiles and smooth surfaces. In this paper, we report on the material and electrical properties of Mg-implanted AlN layers after annealing at various temperatures.

1-μm-thick unintentionally doped AlN (0001) templates were supplied by DOWA Electronics Materials, Ltd., and were grown on 2-inch *c*-plane sapphire substrates by using metal-organic chemical vapor deposition. The concentrations of Si, H, C, and O impurities in the AlN templates were less than 2×10^{17} cm^{-3}. The full width at half maximum value of the X-ray rocking curve for AlN (0002) was less than 150 arcsec. Mg was implanted at room temperature in the as-grown AlN layers at an incident angle of 7° from [0001] by the Ion Technology Center.[6)] The amount and penetration depth of implanted Mg ions were controlled by the implantation dose and ion-beam energy, respectively. The desired box profile of dopants, i.e., Mg concentration of 3×10^{19} cm^{-3} in a 200-nm-deep box profile, was

Accepted Manuscript

optimized by SRIM (stopping and range of ions in matter) Monte-Carlo simulations. The box profile was formed by implanting the Mg ions at ion-beam energies of 90, 40, and 10 keV, where the corresponding dosages were 2.8×10^{14}, 1.6×10^{14}, and 6×10^{13} cm^{-2}. After pumping the chamber to 5×10^{-4} Pa, the Mg-implanted AlN layers were annealed without protective caps at temperatures (T_a) between 1000ºC and 1700ºC for 30 min in a N_2 ambient at 1×10^4 Pa to heal the implantation-induced damage. The susceptor temperature was monitored using a pyrometer.

The surface morphologies of the AlN layers were obtained using a scanning probe microscope. The root-mean-square (RMS) roughness was determined to be over 2 μm ×2 μm. The Mg concentration in the AlN layers was experimentally determined using secondary-ion mass spectrometry (SIMS) performed by the MST Foundation. The detection limit for the Mg concentration was 4×10^{16} cm^{-3}. The depth distribution of point defects in the AlN layers was determined by positron-annihilation spectroscopy (PAS). In AlN, a positron is repelled from an isolated nitrogen vacancy V_N, which is a positively charged defect, because of Coulomb interaction, whereas it is localized in negatively charged defects, such as an aluminum vacancy V_{Al}.[24,28] The low-momentum part was characterized by the S parameter, defined as the number of annihilation events over the energy range of 511±0.76 keV. Doppler broadening spectra of the annihilation radiation were measured with a Ge detector as a function of the incident positron energy E_p using monoenergetic positron beams.

After Mg implantation and subsequent thermal annealing, a Ni (25 nm)/Au (25 nm) metal stack was deposited using an EB evaporation, followed by sintering at temperatures (T_s) between 500ºC and 800ºC for 10 min in an O_2 ambient at 1×10^4 Pa. A 300-nm-deep mesa isolation was obtained by Cl_2-based reactive-ion etching.[29] Current-voltage (I-V) measurements of the Mg-implanted AlN layers were performed between two rectangular contacts of 50 μm × 100 μm at temperatures (T_m) between room temperature and 300ºC by using a semiconductor-device analyzer (Agilent B1500A).

The surface morphologies of the Mg-implanted AlN layers before and after annealing at 1200°C ≤ T_a ≤ 1600°C are shown in Fig. 1. The AlN surfaces before and after annealing at T_a ≤ 1300°C had a small RMS roughness of 0.22±0.04 nm. This highlights the excellent thermal stability of the Mg-implanted AlN layers. The AlN surfaces at T_a = 1200°C and 1300ºC had triangularly shaped islands. We anticipate that Al adatoms created from thermal decomposition form an Al adlayer on the surface, resulting in the formation of two-dimensional islands in excess metal condition.[30,31] The AlN surfaces annealed at T_a ≥

Accepted Manuscript

1400°C increased in RMS roughness as T_a increased. The Si-implanted AlN layer with a total dose of 5×10^{14} cm^{-2} had a smooth surface even after annealing at 1600°C.[32)] Heavy ions produce a relatively high degree of nuclear stopping, causing lattice damage. The Mg implantation may have broken more Al-N bonds in comparison with Si implantation. A smooth surface could be obtained even at a higher T_a by implanting Mg at elevated temperature and by using a protective cap, which can suppress migration of surface atoms during thermal annealing.

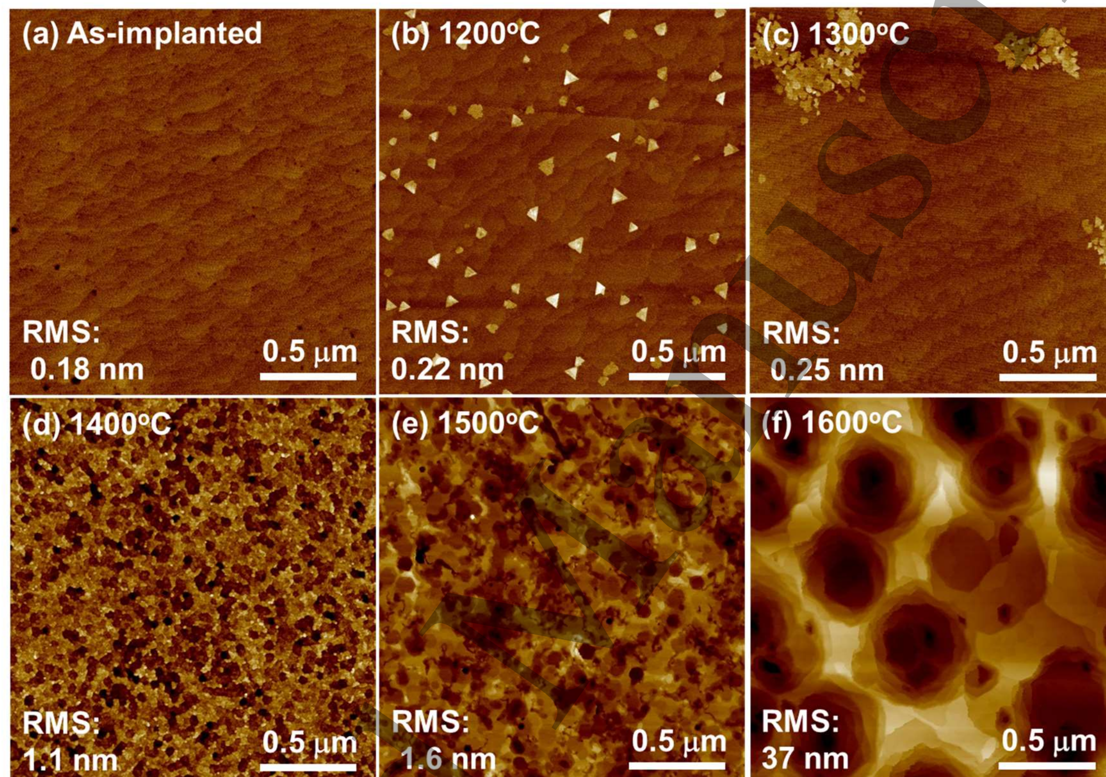

Fig. 1: Surface morphologies of Mg-implanted AlN layers (a) before and after annealing at (b) 1200°C, (c) 1300°C, (d) 1400°C, (e) 1500°C, and (f) 1600°C.

Depth profiles of Mg concentrations in the Mg-implanted AlN layers before and after thermal annealing at various T_a are shown in Fig. 2. The Mg concentration in the as-implanted AlN layer was 2×10^{19} cm^{-3} at 100-nm depth and had a long tail to a 600-nm depth. The discrepancy between the SIMS results and SRIM simulation is attributed to a channeling effect, which allows implanted Mg ions to travel without scattering along [0001]. A larger incident angle than 7° would achieve a steep Mg profile close to the SRIM simulation. The AlN layer at $T_a \leq 1300$°C had a small amount of Mg diffusion, while annealing at $T_a \geq$ 1500°C diffused Mg atoms to a concentration of 2×10^{17} cm^{-3} at the AlN/sapphire interface, which corresponds to the previous result.[24)] After annealing at 1700°C for 30 min, the 670-

Accepted Manuscript

nm-thick AlN layer had decomposed from the surface. The decomposition rate in this case was 22 nm/min, whereas the decomposition rate of a Si-implanted AlN layer with a total dose of 5×10^{14} cm^{-2} at 1800ºC is 8 nm/min.[6)] A large amount of implantation-induced

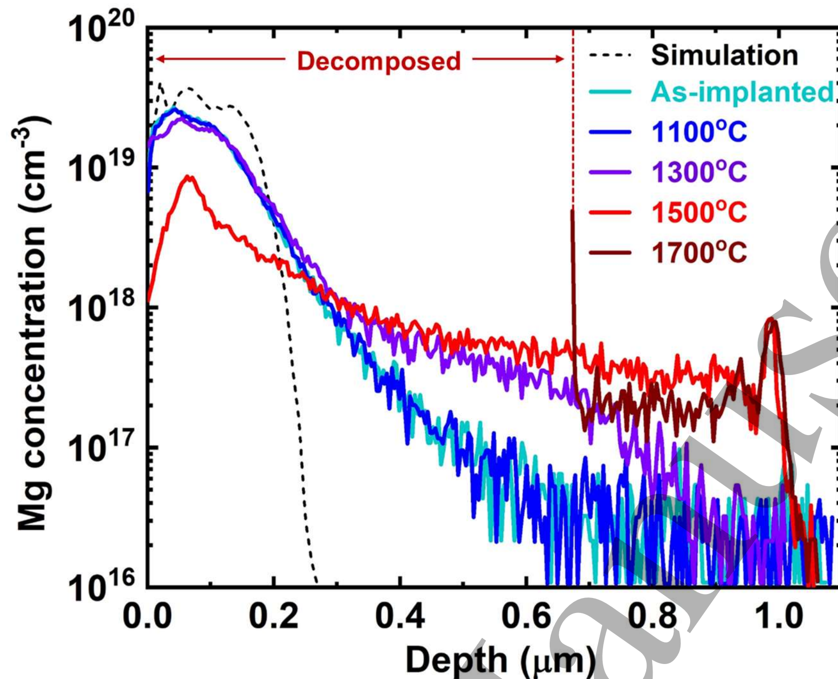

Fig. 2: Depth profiles of Mg atoms in Mg-implanted AlN layers before and after annealing between 1100ºC and 1700ºC. The result of the SRIM simulation is also shown (dashed line). The data of the AlN layer at T_a = 1700°C was shifted to match the depth at the AlN/sapphire interface to the other data.

damage may have enhanced the decomposition rate.

Fig. 3 (a) shows the S values of the Mg-implanted AlN layers in the PAS measurement before and after thermal annealing as a function of E_p. The high S value for E_p < 2 keV is associated with annihilation of positrons at the AlN surface, while the constant S value for E_p =2-10 keV corresponds to annihilation of positrons in the AlN epilayer. The S value of the as-implanted AlN layers was 0.485, which is higher than that of the as-grown AlN layer (=0.470) and the Si-implanted AlN layers (=0.480) with a total dose of 5×10^{14} cm^{-2}.[24)] This indicates that V_{Al}-related defects were introduced by the Mg implantation and that Mg implantation causes more damage than Si implantation does. After annealing at $T_a \leq$ 1300ºC, the S value for E_p =2-7 keV was higher than that for E_p =7-10 keV, suggesting that the implantation-induced defects diffused to the AlN surface and/or new V_{Al}-related defects were generated at the surfaces. The decrease in the S value for E_p > 10 keV is due to

Accepted Manuscript

annihilation of positrons in the sapphire substrate.

The S values at E_p = 3 keV for the Mg-implanted AlN layers before and after thermal annealing are shown as a function of T_a in Fig. 3 (b). The S values of the Mg-implanted AlN layer at T_a = 1200°C and 1300°C were higher than that of the as-implanted AlN layers. The S values for $T_a \geq$ 1400°C dramatically decreased with increasing T_a, indicating that the annihilation of positrons trapped by V_{Al}-related defects was reduced by annealing at $T_a \geq$ 1400°C. The S values for $T_a \geq$ 1500°C were close to that of defect-free AlN (=0.451),[28] implying that the density of V_{Al}-related defects is low enough for AlN devices to operate.

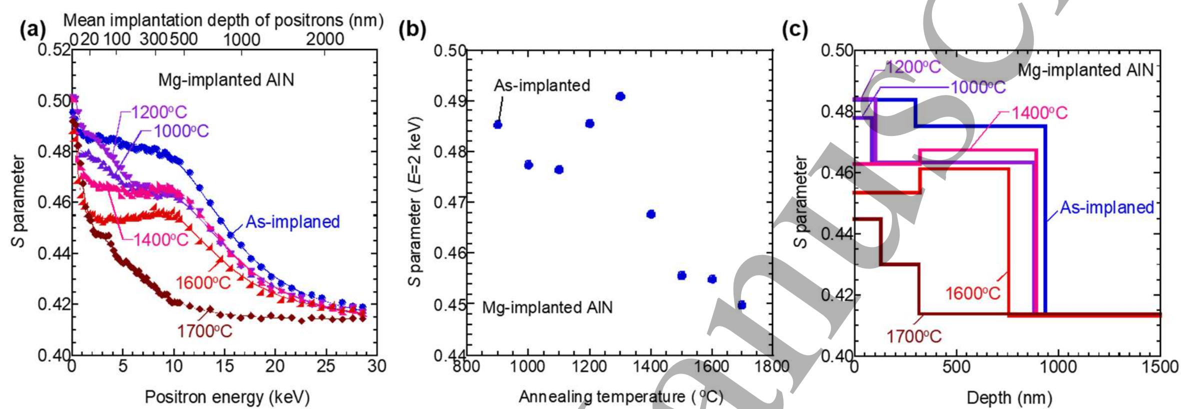

Fig. 3: (a) S parameters as a function of incident positron energy for Mg-implanted AlN layers before and after annealing between 1000°C and 1700°C. Solid curves are fitted to the experimental data. (b) S parameters as a function of annealing temperature for Mg-implanted AlN layers before and after annealing between 1000°C and 1700°C. (c) S depth distributions obtained from analysis of S-E curves for Mg-implanted AlN.

The S–E curves were fitted using $S(E) = S_s F_s(E) + \sum S_i F_i(E)$, where $F_s(E)$ is the fraction of thermalized positrons annihilated at the surface, and $F_i(E)$ the fraction of positrons annihilated in the ith layer with the relation of $F_s(E) + \sum F_i(E) = 1$. S_s and S_i are the S parameter to the annihilation of positrons on the surface and that to the annihilation of positrons in the ith layer, respectively. The region exposed to positrons was divided into three blocks. The solid curves are well fitted to the experimental data, as shown in Fig. 3 (a). The derived depth distributions of the S values for the Mg-implanted AlN layers before and after annealing at various T_a are shown in Fig. 3 (c). The as-implanted, 1000°C-annealed, and 1200°C-annealed AlN layers showed high S values in the first block of ~100-nm depth because of the ion bombardment and high Mg concentration. The S values reduced by annealing at $T_a \geq$ 1400°C. Mg atoms in AlN prefer the substitutional position of the aluminum sublattice, forming substitutional defects (Mg_{Al}).[33] We consider that the low S

Accepted Manuscript

values for $T_a \geq 1400$°C are due to substitution of Mg for V_{Al} and the reduced concentration of V_{Al}-related defects, or self-interstitial-vacancy recombination. The as-implanted AlN layer had a high S value in the second block of ~300-nm depth, which is close to the box profile of Mg implantation, due to the implantation damage. In the first and second blocks, the AlN layers at T_a = 1600°C had a S value of 0.453, which is comparable to that of defect-free AlN.[28] The third block of ~900-nm depth corresponds to the AlN thickness determined by SIMS. We found that the implantation-induced defects were effectively reduced by annealing $T_a \geq 1400$°C.

In the theoretical calculation, the triply positively charged nitrogen vacancy V_N^{3+} and aluminum interstitial Al_i^{3+} have a low formation energy in p-type AlN layers under N-rich conditions and can act as an effective compensating center for shallow acceptors.[34,35] We consider that most of the Mg atoms in AlN lattices diffuse via the kick-out mechanism, in which interstitial-substitutional exchange of Mg atoms creates an Al self-interstitial through the reaction $Mg_i \rightleftarrows Mg_{Al} + Al_i$. The favorable formation of Al_i^{3+} may provide a means of fast Mg diffusion when Mg is implanted in AlN. Additionally, V_N^{3+} deep donors compensate free holes in p-type AlN, reducing the effective acceptor concentrations. Unfortunately, PAS measurements cannot directly detect positively charged defects including Al_i^{3+} and V_N^{3+}. Further investigations using photoluminescence and cathode luminescence will be necessary.

The I-V characteristics of the Mg-implanted AlN layers at T_a = 1500°C are shown in Fig. 4 (a). Here, two Ni/Au contacts with a 2-μm spacing were sintered at various T_s. We confirmed that the Mg-implanted AlN layer was electrically isolated by the bottom UID AlN layer. The currents of the AlN layers at $T_s \leq 500$ °C were under the measurement limit, while those at $T_s \geq 600$ °C were electrically conducting. The AlN layers showed the highest current at T_s = 700°C. The current showed Schottky behavior, indicating a low effective acceptor concentration. Higher Mg concentrations and lower compensation-defect concentrations are needed to achieve ohmic behavior.

The I-V characteristics of the Mg-implanted AlN layers annealed at various T_a are shown in Fig. 4 (b). Here, two Ni/Au contacts were a 2-μm spacing were sintered at 700°C. The AlN layers at $T_a \leq 1300$ °C were insulating, while the AlN layers at T_a = 1400°C and 1500°C were electrically conducting. We found that $T_a \geq 1400$ °C is necessary for electrical activation of the Mg-implanted AlN layer, which is in good agreement with the PAS result. Despite the small S value close to that of the layer annealed at 1500°C, the AlN layer at T_a = 1600°C was insulating, perhaps because of an increase in the contact resistivity by Mg

Accepted Manuscript

diffusion and thermal decomposition of the AlN surfaces.

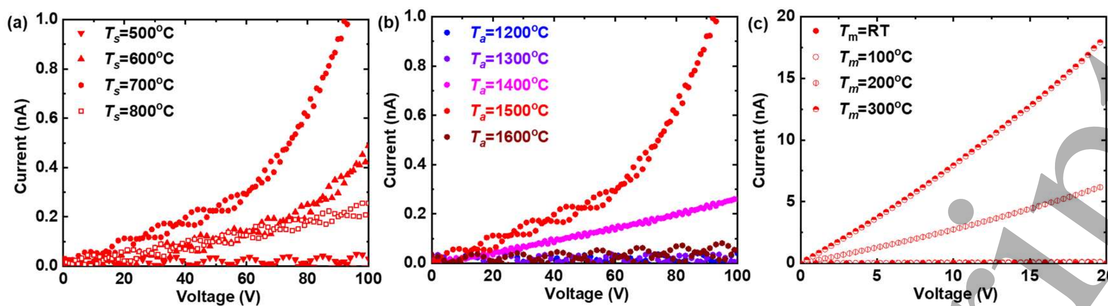

Fig. 4: (a) Room-temperature *I-V* characteristics of Mg-implanted AlN layers after sintering at temperatures between 500°C and 800°C. (b) Room-temperature *I-V* characteristics of Mg-implanted AlN layers after annealing at temperatures between 1200°C and 1600°C. (c) *I-V* characteristics of Mg-implanted AlN layers at temperatures between room temperature and 300°C. All contacts have a spacing of 2 μm.

The *I-V* characteristics of the Mg-implanted AlN layer at T_a = 1500°C are shown in Fig. 4 (c). Here, two Ni/Au contacts with a 2-μm spacing were sintered at 700°C. The currents increased with increasing T_m, reaching 7 nA at a bias of 10 V at T_m = 300°C. However, the carrier type and electrical conduction mechanism of the Mg-implanted AlN layer are unclear. We note that Si-implantation-induced damages with the range of 10^{14}-10^{15} cm^{-2} reduce the electrical conductivity.[32)] Reliable data of the Mg-implanted AlN layer were not obtained from the Hall-effect measurements due to the high resistivity over 10 MΩ. The resistivity should be reduced by increasing the channel thickness and Mg concentration to clarify the carrier type.

The AlN layers at T_a = 1400°C and 1500°C were electrically conducting, and the corresponding PAS measurement showed a reduction in V_{Al}-related defects. We consider that the compensation defects started to be reduced by thermal annealing at T_a ≥1400°C. Meanwhile, the RMS roughness of the AlN surface was increased by annealing at T_a ≥ 1400°C. Mg atoms diffused after annealing at T_a ≥1500°C. We suggest that the ion bombardment forms a high concentration of V_{Al}-related defects, and the thermal annealing causes the lattice of the AlN layer to be disordered. The lattice disorder and threading dislocation in the AlN heteroepitaxial layer on sapphire substrates may lead to the large diffusion length of Mg atoms in the AlN layer, like that of Mg in GaN.[36,37)] We expect that further high-dose Mg implantation at elevated temperature for an AlN homoepitaxial layer and thermal annealing at 1500°C with a protective cap would reduce the compensation defects, Mg diffusion, and surface roughness, and increase the current.

Accepted Manuscript

In conclusion, Mg ions were implanted in 1-μm-thick AlN layers grown on sapphire substrates. The Mg implantation with a total dose of 5×10^{14} cm^{-2} introduced Al-vacancy related defects, which were reduced by annealing at temperatures over 1400°C. Annealing at temperatures over 1500ºC increased the surface roughness and caused Mg diffusion. The Mg-implanted AlN layer annealed at 1500ºC showed the highest current, which was 1.1 nA at a bias of 100 V at room temperature and 7 nA at a bias of 10 V at 300ºC.

Acknowledgements

This work was financially supported by JSPS KAKENHI Grant No. 21H01826 and was carried out at the Nano-Processing Facility at the National Institute of Advanced Industrial Science and Technology and at the open facility at the University of Tsukuba.

References

[1] J. Li, K. B. Nam, M. L. Nakarmi, J. Y. Lin, H. X. Jiang, P. Carrier, and S. Wei, Appl. Phys. Lett. **83**, 5163 (2003).

[2] Y. Taniyasu, M. Kasu, and T. Makimoto, Nature **441**, 325 (2006).

[3] Y. Irokawa, E. Villora, and K. Shimamura, Jpn. J. Appl. Phys. **51**, 040206 (2012).

[4] T. Kinoshita, T. Nagashima, T. Obata, S. Takashima, R. Yamamoto, R. Togashi, Y. Kumagai, R. Schlesser, R. Collazo, A. Koukitu, and Z. Sitar, Appl. Phys. Exp. **8**, 061003 (2015).

[5] H. Fu, X. Huang, H. Chen, Z. Lu, and Y. Zhao, IEEE J. Elect. Dec. Soc. **5**, 518 (2017).

[6] H. Okumura, S. Suihkonen, J. Lemettinen, A. Uedono, Y. Zhang, D. Piedra, and T. Palacios, Jpn. J. Appl. Phys. **57**, 04FR11 (2018).

[7] M. Hiroki, Y. Taniyasu, and K. Kumakura, IEEE Elect. Dev. Lett. **43**, 350 (2022).

[8] P. Reddy, I. Bryan, Z. Bryan, J. Tweedie, R. Kirste, R. Collazo, and Z. Sitar, J. Appl. Phys. **116**, 194503 (2014).

[9] T. Maeda, R. Page, K. Nomoto, M. Toita, H. Xing, and D. Jena, Appl. Phys. Exp. **15**, 061007 (2022).

[10] P. Boguslawski and J. Bernhole, Phys. Rev. B **56**, 9496 (1997).

[11] K. B. Nam, M. L. Nakarmi, J. Li, J. Y. Lin, and H. X. Jiang, Appl. Phys. Lett. **83**, 878 (2003).

[12] N. T. Son, M. Bickermann, and E. Janzen, Appl. Phys. Lett. **98**, 092104 (2011).

[13] T. Ive, O. Brandt, H. Kostial, K. J. Friendland, L. Daweritz, and K. H. Ploog, Appl. Phys. Lett. **86**, 024106 (2005).

Accepted Manuscript

[14] I. Bryan, Z. Bryan, S. Washiyama, P. Reddy, B. Gaddy, B. Sarkar, M. H. Breckenridge, Q. Guo, M. Bobea, J. Tweedie, S. Mita, D. Irving, R. Collazo, and Z. Sitar, Appl. Phys. Lett. **112**, 062102 (2018).

[15] N. Yafune, S. Hashimoto, K. Akita, Y. Yamamoto, and M. Kuzuhara, Jpn. J. Appl. Phys. **50**, 100202 (2011).

[16] S. Bajaj, F. Akyol, S. Krishnamoorthy, Y. Zhang, and S. Rajan, Appl. Phys. Lett. **109**, 133508 (2016).

[17] M. Hiroki and K. Kumakura, Appl. Phys. Lett. **115**, 192104 (2019).

[18] A. Baca, A. M. Armstron, A. Allerman, E. Douglas, C. Sanchez, M. King, M. coltrin, T. Fortune, and R. Kaplar, Appl. Phys. Lett. **109**, 033509 (2016).

[19] I. Abid, J. Mehta, Y. Cordier, J. Derluyn, S. Degroote, H. Miyake, and F. Medjdoub, Electronics **10**, 635 (2021).

[20] R. Maeda, K. Ueno, A. Kobayashi, and H. Fujioka, Appl. Phys. Exp. **15**, 031002 (2022).

[21] K. Kishimoto, M. Funato, and Y. Kawakami, Appl. Phys. Exp. **13**, 015512 (2020).

[22] M. Kanechika and T. Kachi, Appl. Phys. Lett. **88**, 202106 (2006).

[23] M. H. Breckenridge, P. Bagheri, Q. Guo, B. Sarkar, D. Khachariya, S. Pavlidis, J. Tweedie, R. Kirste, S. Mita, P. Reddy, R. Collazo, and Z. Sitar, Appl. Phys. Lett. **118**, 112104 (2021).

[24] H. Okumura, Y. Watanabe, T. Shibata, K. Yoshizawa, A. Uedono, H. Tokunaga, S. Koseki, T. Arimura, S. Suihkonen, and T. Palacios, Jpn. J. Appl. Phys. **61**, 026501 (2022).

[25] H. Ahmad, J. Lindemuth, Z. Engel, C. M. Matthews, T. M. McCrone, and W. A. Doolittle, Advanced Mat. **33**, 2104497 (2021).

[26] N. Napal, M. Nakarmi, H. Jang, J. Lin, and H. Jiang, Appl. Phys. Lett. **89**, 192111 (2006).

[27] P. Bagheri, A. Klump, S. Washiyama, M. Breckenridge, J. Kim, Y. Guan, D. Khachariya, C. Garcia, B. Sarkar, S. Rathkanthiwar, P. Reddy, S. Mita, R. Kirste, R. Collazo, and Z. Sitar, Appl. Phys. Lett. **120**, 082102 (2022).

[28] A. Uedono, K. Shojiki, K. Uesugi, S. Chichibu, S. Ishibashi, M. Dickmann, W. Egger, C. Hugenschmidt, and H. Miyake, J. Appl. Phys. **128**, 085704 (2020).

[29] H. Okumura, Jpn. J. Appl. Phys. **58**, 026502 (2019).

[30] L.X. Zheng, M. H. Xie, S. M. Seutter, S. H. Cheung, and S. Y. Tong, Phys. Rev. Lett. **85**, 2352 (2000).

[31] H. Okumura, B. M. McSkimming, T. Huault, C. Chaix, and J. S. Speck, Appl. Phys. Lett. **104**, 012111 (2014).

Accepted Manuscript

[32] H. Okumura, S. Suihkonen, J. Lemettinen, A. Uedono, and T. Palacios, Ext. Abstr. Int. Conf. Solid State Devices and Materials, 2017, N-2-06, p. 641.

[33] L. M. Amorim, U. Wahl, L. Pereira, S. Decoster, D. Silva, M. Silva, A. Gottberg, K. Temst, and A. Vantomme, Appl. Phys. Lett. **103**, 262102 (2013).

[34] C. Stampfl and C. G. Van de Walle, Phys. Rev. B **65**, 155212 (2002).

[35] Y. Zhang, W. Liu, and H. Niu, Phys. Rev. B **77**, 035201 (2008).

[36] K. Harafuji and K. Kawamura Jpn. J. Appl. Phys. **44**, 6495 (2005).

[37] T. Narita, A. Uedono, and T. Kachi, Physica Status Solidi B, 2200235 (2022).

Accepted Manuscript